Available online at http://www.journalcra.com

International Journal of Current Research
Vol. 11, Issue, 08, pp.6459-6464, August, 2019

DOI: https://doi.org/10.24941/ijcr.36439.08.2019

ISSN: 0975-833X

INTERNATIONAL JOURNAL OF CURRENT RESEARCH

RESEARCH ARTICLE

PARAMETRIC GEOMETRIC MODELING OF THE THEORETICAL PROFILES OF WORM AND HOLLOW WHEELS

[1]Komlan A. KASSEGNE, [1]Kokou F. WOTODZO, [2]Folly K. ABEVI, [1]Sonnou TIEM and [3]Kossi NAPO

[1]ENSI – Université de Lomé, Togo
[2]INSA de Toulouse, France
[3]FDS – Université de Lomé, Togo

ARTICLE INFO

Article History:
Received 18th May, 2019
Received in revised form
09th June, 2019
Accepted 11th July, 2019
Published online 31st August, 2019

Key Words:

Profile, Parameterization, Hollowwheel, Wormgear, Screw gear.

***Corresponding author:** Komlan A. KASSEGNE

ABSTRACT

A parametric model to represent the profiles of ZA, ZI and ZK-types worms and a hollow wheel in the transverse plane (plane normal to the axis of the worm) has been developed, based on their characteristics. The profiles represented by a relatively fine meshing are more representative and can be used to generate wheels and worms more easily under the CAD and the finite element software's. As a result, these models can be useful in rapid prototyping to manufacture worm gears according to the perfect theoretical model.

***Citation: Komlan A. KASSEGNE, Kokou F. WOTODZO, Folly K. ABEVI, Sonnou TIEM and Kossi NAPO,* 2019.** "Parametric geometric modeling of the theoretical profiles of worm and hollow wheels", *International Journal of Current Research*, 11, (08), 6459-6464.

INTRODUCTION

Worm gears are used to transmit a torque between two non-coplanar axes, usually at a 90° angle between them, especially in the case of transmission with a high speed ratio. They are often used in divisors. Among them, the most widespread remains the worm gear with a hollow wheel. Several modeling works of profiles and surfaces [15-18] have been carried out based on the kinematic conditions of cutting. The authors take into account the interaction between the tool and the work piece to determine the equations of the surfaces and profiles. These models, if it is interest when machining metal materials, may be ineffective when dealing with plastic worm gear molding or rapid prototyping.

WORM MODELING

The distinction of the worm is based on the nature of their profile in the axial plane. There are four types: ZA worm (trapezoidal thread) (Fig.1), ZK worm (circular thread), ZI worm (involute thread), ZN worm (globular worm). By adopting a complex notation, the equation of their profile in the axial plane(O, O_y, O_z) is given by the relation Eq.1 where $s_{m,x}$ isthe axial thickness of a net at the radius r_m.

$$z_{m,x} = \tfrac{1}{2} s_{m,x} + i.r_m = r_m e^{i\phi_m} \quad (1)$$

A point M of the axial profile of affix $z_{m,x}$, has in the (apparent) normal plane an affix $z_{m,p}$ whose expression is given by the relation Eq.2 where $s_{m,p}$ is the apparent thickness of a net at the radius r_m.

$$z_{m,p} = -\tfrac{1}{2} s_{m,p} + i.(r_m \cos(\theta_m)) = r_m e^{i\left(\theta_m + \frac{\pi}{2}\right)} \quad (2)$$

To determine the apparent profile of a worm is to determine the polar angle θ_m. Equation Eq.3 gives the expression:

$$\theta_m = \frac{\pi}{z.p_x}\left(s_{m,x}\right) \quad (3)$$

The distinction between the worms ZA, ZI and ZK is related to the expression of $s_{m,x}$ which is explained afterwards, for each of these three types of worm.

Trapezoidal profile screw (type ZA)

The type ZA worm has in the axial section a rectilinear profile determined by the axial pressure angle α_x. In the normal section to the axis, this worm has a curved profile which despite its appearance is not a involute of a circle. This profile is called Archimedes spiral.

$$s_{m,x} = s_{a,x} + 2(r_a - r_m)\tan\alpha_x \tag{4}$$

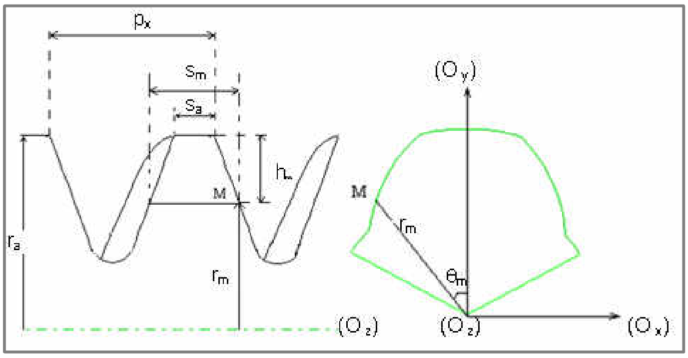

Figure 1. Representation of a 5-thread trapezoidal screw cutter

Circular profile worm (type ZK)

The axial profile of the worm ZK is a portion of a circle defined by its center $O = (x_0, y_0)$ and its curved radius R_o . The axial thickness and the equation of the normal profile are given by the following relation.

$$s_{m,x} = 2\left(y_o + \sqrt{R_o^2 - (r_m + x_o)^2} \right) \tag{5}$$

Worm with involute profile (ZI)

The apparent section of the worm has an involute profile of a circle. The developable helical worm can therefore be likened toa cylindrical wheel with helical teeth of helix angle β_b (Eq.6). The axial section, even if it seems to be rectilinear, is always convex [14].

$$\beta_b = \arctan\left(\frac{d_{b1}}{z_1 m_x}\right) = \arctan\left(\frac{d_1 \cos\alpha_x}{z_1 m_x}\right) \tag{6}$$

The section of the threads (Figure 2) of the screw by a plane parallel to the axial plane and tangential to the base cylinder gives a rectilinear profile whose pressure angle α is given by the relation Eq.7.

$$\alpha = \frac{\pi}{2} - \beta_b \tag{7}$$

This straight profile is a fundamental property for developable helical worms. It represents the generating tangent of the net. A point M of the axial profile corresponds to a radius r_m, an angle of incidence α_m and an axial thickness $s_{m,x}$ (Eq.8), has for affix z_m .

$$s_{m,x} = p_z \frac{inv\alpha_m}{\pi} \tag{8}$$

Profile representation procedure

The representation of the normal profile is done according to the algorithm described in appendix 1. The geometric quality is then function of the number n_d of points M chosen: it is the constant of discretization or the parameter of mesh of the profile. The bigger is n_d , the better the accuracy.

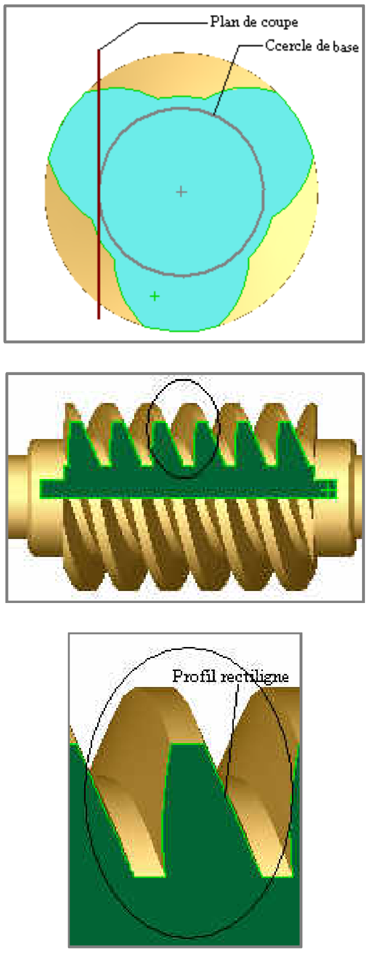

Figure 2. Section of a ZI worm

MODELING HOLLOW WHEELS

The modeling of the hollow worm wheel is very complex because the parameters and characteristics are defined only in the median plane of the wheel (axial plane of the screw). The difficulties also lie in the non-uniformity of the profiles according to the various planes normal to the axis of the hollow

Determination of the profile in a normal plane wheel

The study of a worm gear is reduced in the axial plane to a gear rack. Therefore, the conjugate profile of the wheel in this plane is the involute corresponding to this rack. The profile is determined as if it were an ordinary helical wheel using the apparent parameters. The apparent pressure angle of the hollow wheel is equal to the axial pressure angle of the conjugate worm. In addition, the cutting of the wheel is usually without interference because of its large number of teeth.

$$\Gamma = \Gamma_i \cup \Gamma_t \tag{9}$$

The profile Γ (Eq.9) of a wheel then consists of a involute (involute of circle) Γ_i, and a trochoïde (connection at the foot of tooth), Γ_t .

Principle of parametrization: The method used for the modeling of the hollow width wheel $b$is based on the determination of any profile Γ_q in any plane normal to the axis of the wheel.

$$(P_q): z_q = k \ , \ |k| = b_q \leq b \tag{10}$$

Table 1: Geometric characteristics of a worm gear [3, 14]

GRANDEURS	VIS	ROUE
Axial module (screw) or apparent (wheel)	m_x	
Number of nets or teeth	z_1	z_2
Helix angle	β_1	β_2
offset	$x = \omega_0 \varepsilon$	$x = \omega_0 (1-\varepsilon)$
Real module	$m_n = m_x \sin \beta_1$	
Axial pressure angle (screw) or apparent (wheel)	α_x	
Not axial (screw) or apparent (wheel)	$p_x = \pi m_x$	
Helical step	$p_{z1} = z_1 p_x$	$p_{z2} = z_2 p_x$
Normal system with $\beta_1 > 75°$		
Reference protrusion	$h_a = m_x$	
Hollow reference	$h_f = 1.2 m_x$	
Tooth height	$h = 2.2 m_x$	
Empty at the bottom of the tooth	$c = 0.2 m_x$	
Normal system with $\beta_1 < 75°$		
Reference protrusion	$h_a = m_n$	$h_a = m_n$
Hollow reference	$h_f = 1.2 m_n$	$h_f = 1.2 m_n$
Tooth height	$h = 2.2 m_n$	$h = 2.2 m_n$
Empty at the bottom of the tooth	$c = 0.2 m_n$	$c = 0.2 m_n$
Reference primitive diameter	$d_1 = q m_x$	$d_2 = (z_2 + 2x) m_x$
Head diameter	$d_{a1} = d_1 + 2h_a$	$d_{a2} = d_2 + 2h_a$
Foot diameter	$d_{f1} = d_1 - 2h_f$	$d_{f2} = d_2 - 2h_f$
External diameter		$d_e = d_a + m_x$
Base diameter (ZI screws only)	$d_b = d_1 \cos \alpha_x$	

Let us denote by $(\Delta)$the axis of the worm and by P_q any plane of equation Eq.10. P_q is normal to the $(O_2 z)$axis of the wheel and parallel to the $(O_1 x)$ axis of the worm. Let us cut a tooth from the hollow wheel by a plane P_m containing Δ and secant to the plane P_q. Let us denote by P_m an axial plane of the worm. Let M_q the intersection point of the planes P_q, P_m and a side of the tooth, M_0 its counterpart in the median plane P_0 of the wheel (Figure 3) and b_q the spacing between P_q and P_0. To determine the parametric equation of the profile of the hollow wheel, is to look for the affix $z_{m,q}$ (Eq.11) of the point M_q in the plane P_q related to an orthonormal coordinate system $(O_q, \vec{e}_i, \vec{e}_j)$. It involves finding, implicitly, the polar coordinates $R_{m,q}$ and $\partial_{m,q}$ defining any point M_q of the profile.

$$z_{m,q} = R_{m,q}\left(\sin(\partial_{m,q}) + i\cos(\partial_{m,q})\right) = R_{m,q} e^{-i\left(\partial_{m,q} + \frac{\pi}{2}\right)} \tag{11}$$

Thus, it would be possible for example to easily find the equation of Γ_q in the three particular planes that are the median plane P_0 (reference plane), the intermediate plane or "sandwich" P_1 (Figure3) and the outer plane P_3.

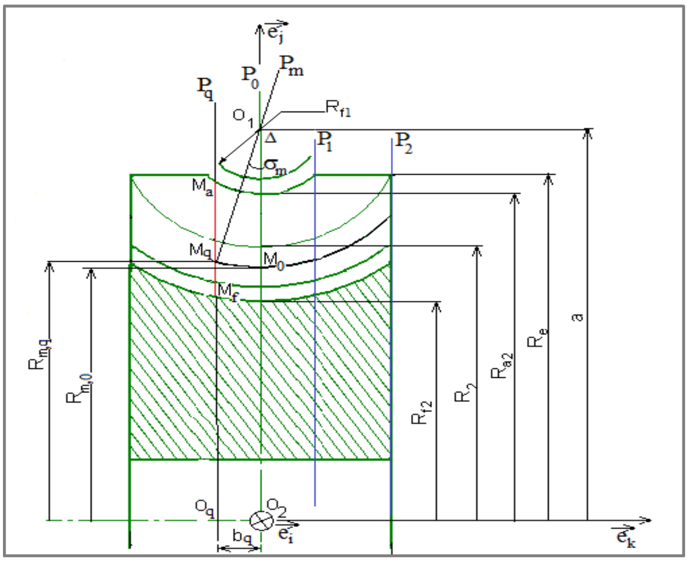

Figure 3. Cutting a hollow wheel tooth

Determination of involute: The plane P_m forms an angle $\sigma_{m,q}$ with the plane P_q. By noting $\sigma_{inv,q}$ the angle that the plane P_m makes at the point of maximum clearance $M_{d,q}$, and $\sigma_{a,q}$ the angle that the plane P_m makes at the point of the tooth's head $M_{a,q}$, we can write the relations Eqs.12, 13 and 14, where $H(b_q - b_1)$ is the function of Heaviside.

$$\sigma_{inv,q} = \arcsin\left(\frac{b_q}{a - R_{inv,q}}\right) \tag{12}$$

$$R_{a,q} = a - \left(\frac{b_q}{\tan \sigma_{m,q}}\right)\left[1 - H(b_q - b_1)\right] + (R_e - a) H(b_q - b_1) \tag{13}$$

$$\sigma_{a,q} = \arcsin\left(\frac{b_q}{a - R_{a,q}}\right) \tag{14}$$

Moreover, the conjugate profile $\Gamma_{i,m}$ of the wheel in the plane P_m is identical to the profile $\Gamma_{i,0}$ in the median plane P_0 of the wheel. Every point M_0 of the profile $\Gamma_{i,0}$ has an angle of incidence $\alpha_{m,0}$ (Eq.15) and is marked by its polar angle $\theta_{m,0}$ (Eq.16).

$$\alpha_{m,0} = \arccos\left(\frac{R_{b2}}{R_{m,0}}\right) \quad (15)$$

$$\theta_{m,0} = inv(\alpha_{t,0}) - inv(\alpha_{m,0}) \quad (16)$$

Considering the angle $\sigma_{m,q}$ that the plane P_m makes with the median plane P_0 and the distance b_q between P_q and P_0, we can determine the radius $R_{m,0}$ (Eq.20) of the center of the wheel at the homologous point M_0 and subsequently the coordinates of the point M_q.

$$R_{m,0} = R_{a2} - \left(\frac{b_q}{\sin\sigma_{m,q}} - (R_f + c)\right) \quad (17)$$

$$\psi_q = \frac{b_q}{R_2}\tan(\beta_2) \quad (18)$$

In the plane P_q, one can note the existence of the axis of symmetry $(O_q, \vec{e}_q)$ to the profile. $(O_q, \vec{e}_q)$ and $(O_q, \vec{e}_j)$ are such as $(\vec{e}_q, \vec{e}_j) = \psi_q$ (Eq.18). Since the tooth thickness is constant, the axial thickness $s_{m,q}$ in the plane P_q at the point M_q is identical to the thickness $s_{m,0}$ (Eq.19) at the point M_0 in the reference plane P_0. We then deduce the abscissa $x_{m,q}$ of the points M_q of the profile by the relation Eq.20.

$$s_{m,q} = s_{m,0} = R_{m,0}\sin\left(inv(\alpha_{t,0}) - inv(\alpha_{m,0})\right)$$
(19)

$$x_{m,q} = R_{m,0}\sin\left(inv(\alpha_{t,0}) - inv(\alpha_{m,0}) + \psi_q\right) \quad (20)$$

The angle $\partial_{m,q}$ that the radius $R_{m,q}$ (Eq.21) makes with the axis $(O_q, \vec{e}_j)$ in the plane P_q is given by the relation Eq.22.

$$R_{m,q} = a - \frac{b_q}{\tan(\sigma_{m,q})} \quad (21)$$

$$\partial_{m,q} = \arcsin\left(\frac{x_{m,q}}{R_{m,q}}\right) = \left(\frac{R_{m,0}\sin\left(inv(\alpha_{t,0}) - inv(\alpha_{m,0}) + \psi_q\right)}{a - \dfrac{b_q}{\tan\sigma_{m,q}}}\right) \quad (22)$$

The polar coordinates $R_{m,q}$ and $\partial_{m,q}$ being defined, the affix $z_{m,q}$ of the point M_q can then be determined with the relation Eq.11.

Determination of the trochoid: The principle of determining the points of the profile $\Gamma_{t,q}$ corresponding to the trochoid is the same as that of the determination of the points corresponding to the involute $\Gamma_{i,q}$. Every point M_0 of the trochoid in the plane P_0 is marked by its radius $R_{m,0}$ and its angle $\theta_{m,0}$ compared to axis $(O_0, \vec{e}_0)$ defined by the relations Eqs.17 and 23.

$$\theta_{m,0} = -\delta_{m,0} + \delta_{\max,0} + inv(\alpha_{t,0}) \quad (23)$$

Note that the expression of $\theta_{m,0}$ is obviously different from that of the involute. It depends on the angle of incidence $\delta_{m,0}$ of the point M_0 of the trochoid translated by the relation Eq.24.

$$\delta_{m,0} = \arctan\left(\sqrt{\left[\left(\frac{\varphi_{m,0}}{0.5-K}\right)^2 - 1\right]}\right) - 2\pi\sqrt{\varphi_{m,0}^2 - (0.5-K)} \quad (24)$$

The variables K and $\delta_{\max,0}$ are the parameters of G. Henriot [3, 4] whose expressions are mentioned in the appendix. As a result, for every point M_q of $\Gamma_{t,q}$ in the plane P_q, its abscissa $x_{m,q}$ is determined by equation Eq.25.

$$x_{m,q} = R_{m,q}\sin(\theta_{m,q}) = R_{m,q}\sin\left(-\delta_{m,0} + \delta_{\max,0} + inv(\alpha_{t,0}) + \psi_q\right) \quad (25)$$

The expression of the ray $R_{m,q}$ in P_q remains the same, therefore identical to the relation Eq.21. It is then possible to determine $\partial_{m,q}$ the angle that this ray makes with the axis $(O_q, \vec{e}_j)$ by the relation Eq.26. By substituting of $x_{m,q}$ with its expression, we deduce the relation:

$$\partial_{m,q} = \arcsin\left(\frac{R_{m,0}\sin\left(-\delta_{m,0} + \delta_{\max,0} + inv(\alpha_{t,0}) + \psi_q\right)}{R_{m,q}}\right) \quad (26)$$

Procedure for obtaining the profile of the hollow wheel in the plan P_q

It has just been shown that the profile Γ_q of the hollow wheel is the locus of the points M_q in the plan P_q, which goes from the point of the head $M_{a,q}$ to the point of the foot $M_{f,q}$, passing through the point of clearance $M_{d,q}$. Numerically, Γ_q is obtained by varying the angle $\sigma_{m,q}$ in the range of values $\left[\sigma_{a,q}, \sigma_{inv,q}\right] \cup \left[\sigma_{inv,q}, \sigma_{f,q}\right]$. We can then write a procedure as explained in appendix 2.

APPLICATIONS

The procedures developed above have been implemented in a VB application (Figure 4) interfaced with the Solid Works CAD software. This coupling makes it easier to generate both the profiles (Figures 5 and 6) and the components (Figure 8) of the gear with good geometric accuracy by inserting a point file combined with other features.

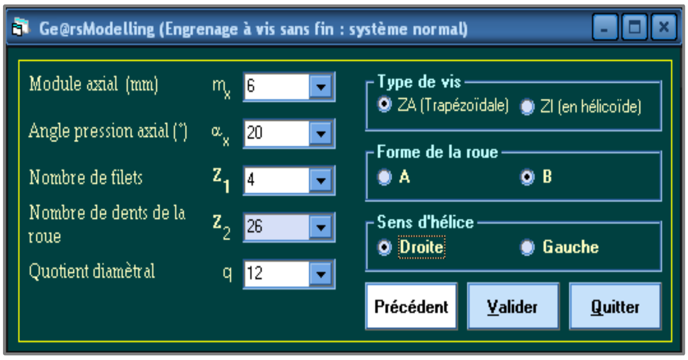

Figure 4. Graphical interface under VB

Figure 5 illustrates the profile in the normal plane of a hollow wheel tooth for both normal and deported teeth (positive and negative deports).

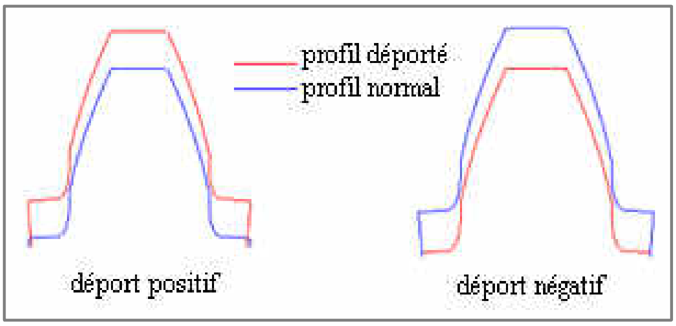

Figure 5. Profile of a hollow wheel tooth

Figure 6 illustrates the profile of a thread of a worm for both normal and deported teeth (positive and negative deports).

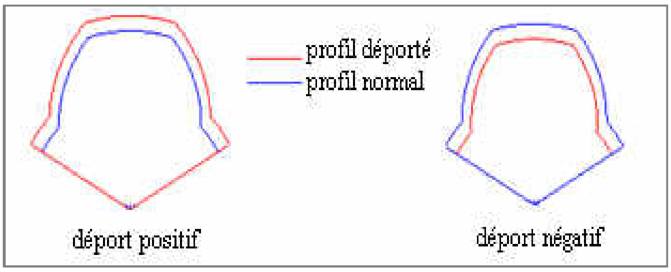

Figure 6. Normal profile of a worm net

Figure 7 compares the axial profiles of screws ZA and ZI with each other for the same characteristics. There is a slight gap between the two profiles at the root of the net as they seem to be confused beyond. In reality, both profiles are tangent to the primitive point.

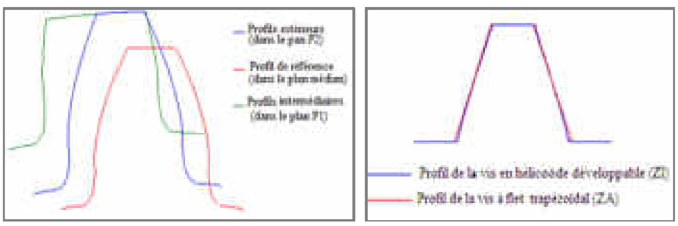

Figure 7: Axial profiles of screws ZA, ZIwith $q = 12$; $\alpha_x = 20°$; $m_x = 6$; $z_1 = 4$

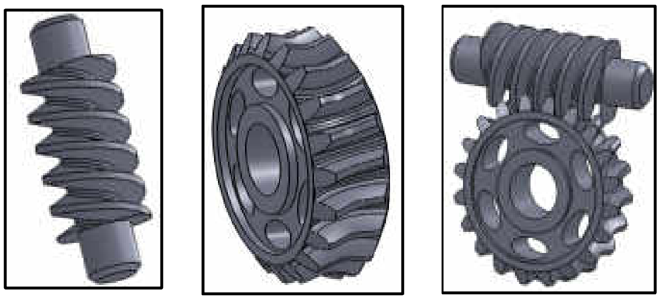

Figure 8: Screw gear under SolidWorks $m_x = 4$; $\alpha_x = 20°$; $q = 8$; $z_1 = 2$; $z_2 = 20$.

Conclusion

Due to the knowledge of the axial parameters of a worm gear, we have modeled the apparent profiles of the worm and hollow wheels. As a result, CAD models were more easily and faithfully generated by the theory of software interaction. It is then possible to envisage later a thermo mechanical analysis of worm gears relating to contact problems by a finite element analysis. Another interest of this work is the possibility to be able to realize in series worm and hollow wheels, with a good geometric precision, by rapid prototyping.

REFERENCES

[1] Abevi F. 2006. “Modélisation géométrique paramétrée CAO sous SolidWorks des engrenages parallèles et des engrenages concourants”, Mémoire d’Ingénieur, ENSI Université de Lomé, Togo.

[2] Chung M.Y. and Shaw D. 2007. “Parametric study of dynamics of worm and worm gear set under suddenly applied rotating angle”, *Journal of sound and vibration* Vol. 304, 246-262.

[3] Henriot G. 1983. “Traité théorique et pratique des engrenages”, Tome1 : Théorie et technologie, 5ème édition ; Dunod, Bordas, Paris.

[4] Henriot G. 1983. “Traité théorique et pratique des engrenages”, Tome2 : Etude complète du matériel, 5ème édition ; Dunod, Bordas, Paris.

[5] Hiltcher Y. *et al.* 2006. “Numerical simulation and optimisation of worm gear cutting”, *Mechanism and Machine Theory,* Vol. 41, 1090-1110.

[6] Koffi D. *et al.* 2005. “ Modélisation géométrique paramétrée CAO sous Solid Works des profils d’engrenages cylindriques en plastique à dentures droites pour l’analyse du comportement mécanique”, *Revue Internationale d’Ingénierie Numérique*, Vol 1 n°3.

[7] Kuan-Yu C. and Chung-Biau T. 2009. “Mathematical model and worm wheel tooth working surfaces of the ZN-type hourglass worm gear set”, *Mechanism and Machine Theory,* Vol. 44, pp. 1701-1712.

[8] Lampoh K. 2006. “Modélisation géométrique paramétrée CAO sous SolidWorks des engrenages gauches et des engrenages concourants”, Mémoire d’Ingénieur, ENSI Université de Lomé, Togo.

[9] Litvin F.L. and De Donno M. 1998. “Computerized design and generation of modified spiroid worm-gear drive with low transmission errors and stabilized bearing contact”, *Computer methods in applied mechanics and engineering* Vol. 162, pp. 187-201.

[10] Litvin F.L. *et al.* 2000. "Computerized design, generation and simulation of meshing and contact of face worm-gear drive", *Computer methods in applied mechanics and engineering,* Vol. 189, pp. 785-801.
[11] Litvin F.L. *et al.* 2007. "Design, simulation of meshing, and contact stresses for an improved worm gear drive" *Mechanism and Machine Theory* Vol. 42, pp. 940-959.
[12] Liu C.C. *et al.* 2006. "Meshing simulations of the worm gear cut by a staight-edged flyblade and the ZK-type worm with a non-90° crossing angle", *Mechanism and Machine Theory,* Vol. 41, pp. 987-1002.
[13] Mohan L.,V. and Shunmgam M.S. 2009. "Geometrical aspects of double enveloping worm gear drive" *Mechanism and Machine Theory* Vol. 44, pp. 2053-2065.
[14] Scharwzman M. 1983. "Eléments de machines", Technique et Documentation (Lavoisier),
[15] Simon V. 2006. "Influence of tooth errors and shaft misalignments on loaded tooth contact in cylindrical worm gears", *Mechanism and Machine Theory,* Vol. 41, pp. 707-724.
[16] Tsay C.-B. *et al.* 1995. "A mathematical model of the ZE-type worm gear set", *Mechanism and Machine Theory* Vol. 30, pp. 777-789.
[17] Wang S. *et al.* 2002. "Tooth contact analysis of toroidal involute worm mating with involute helical gear",*Mechanism and Machine Theory* Vol. 37, pp. 685-691.
[18] Yeh T.J. and Wu F.-K. 2007. "Modelling and robust control of worm-gear driven systems", *Simulation Modelling Practice and Theory,* Vol. 17, pp. 767-777.

APENDIX

Apendix1: Procedure for representing an apparent worm profile [8]

Beginning

$$\lambda_d = \frac{1}{n_d}$$

For $u_m \in [0,1]$, repeat :

$$r_m = r_a - u_m h$$

$$\theta_m = \frac{\pi}{z.p_x}\left(s_{m,x}\right)$$

$$z_m = r_m e^{i\theta_m}$$

$$u_{m+1} = u_m + \lambda_d$$

End

Apendix 2: Procedure for representing the profile of a hollow wheel [1, 8].

Beginning

{Obtaining the involute}

$$\lambda_d = \frac{1}{n_d}$$

For $u_m \in [0,1]$, repeat :

$$\sigma_{m,q} = u_{\cdot m}\left(\sigma_{a,q} - \sigma_{inv,q}\right) + \sigma_{inv,q}$$

$$R_{m,0} = R_{a2} - \left(\frac{b_q}{\sin\sigma_{m,q}} - \left(R_f + c\right)\right)$$

$$R_{m,q} = a - \frac{b_q}{\tan\sigma_{m,q}}$$

$$\partial_{m,q} = \left(\frac{R_{m,0}\sin\left(inv\left(\alpha_{t,0}\right) - inv\left(\alpha_{m,0}\right) + \psi_q\right)}{R_{m,q}}\right)$$

$$z_{m,q} = R_{m,q} e^{-i\left(\partial_{m,q} + \frac{\pi}{2}\right)}$$

$$u_m = u_m + \lambda_d$$

{Obtaining the trochoid}

$$\lambda_v = \frac{1}{n_v}$$

$$K = \frac{R_2 - R_{f2}}{m_x z_2}$$

$$\varphi_{inv,0} = \sqrt{\frac{0.5 - K}{2}}$$

$$\delta_{\max,0} = \delta_{m,0}\left(\varphi_{inv,0}\right) = \arctan\left(\sqrt{\left[\left(\frac{\varphi_{inv,0}}{0.5 - K}\right)^2 - 1\right]}\right) - 2\pi\sqrt{\varphi_{inv,0}^2 - (0.5 - K)}$$

For $u_m \in [0,1]$, repeat :

$$\sigma_{m,q} = u_{\cdot m}\left(\sigma_{f,q} - \sigma_{inv,q}\right) + \sigma_{inv,q}$$

$$\varphi_{m,0} = \frac{R_{m,0}}{2R_2}$$

$$\delta_{m,0} = \arctan\left(\sqrt{\left[\left(\frac{\varphi_{m,0}}{0.5 - K}\right)^2 - 1\right]}\right) - 2\pi\sqrt{\varphi_{m,0}^2 - (0.5 - K)}$$

$$R_{m,q} = a - \frac{b_q}{\tan\sigma_{m,q}}$$

$$\partial_{m,q} = \arcsin\left(\frac{R_{m,0}\sin\left(-\delta_{m,0} + \delta_{\max,0} + inv\left(\alpha_{t,0}\right) + \psi_q\right)}{R_{m,q}}\right)$$

$$z_{m,q} = R_{m,q} e^{-i\left(\partial_{m,q} + \frac{\pi}{2}\right)}$$

$$u_m = u_m + \lambda_v$$

End

****